This article is a *Plant Cell* Advance Online Publication. The date of its first appearance online is the official date of publication. The article has been edited and the authors have corrected proofs, but minor changes could be made before the final version is published. Posting this version online reduces the time to publication by several weeks.

cis-Regulatory Elements and Chromatin State Coordinately Control Temporal and Spatial Expression of *FLOWERING LOCUS T* in *Arabidopsis* [W][OA]

Jessika Adrian,[1] Sara Farrona,[1] Julia J. Reimer, Maria C. Albani, George Coupland, and Franziska Turck[2]

Max Planck Institute for Plant Breeding Research, 50829 Koeln, Germany

Flowering time of summer annual *Arabidopsis thaliana* accessions is largely determined by the timing of *FLOWERING LOCUS T* (*FT*) expression in the leaf vasculature. To understand the complex interplay between activating and repressive inputs controlling flowering through *FT*, *cis*-regulatory sequences of *FT* were identified in this study. A proximal and an ~5-kb upstream promoter region containing highly conserved sequence blocks were found to be essential for *FT* activation by CONSTANS (CO). Chromatin-associated protein complexes add another layer to *FT* regulation. In plants constitutively overexpressing *CO*, changes in chromatin status, such as a decrease in binding of LIKE HETEROCHROMATIN PROTEIN1 (LHP1) and increased acetylation of H3K9 and K14, were observed throughout the *FT* locus, although these changes appear to be a consequence of *FT* upregulation and not a prerequisite for activation. Binding of LHP1 was required to repress enhancer elements located between the CO-controlled regions. By contrast, the distal and proximal promoter sequences required for *FT* activation coincide with locally LHP1 and H3K27me3 depleted chromatin, indicating that chromatin status facilitates the accessibility of transcription factors to *FT*. Therefore, distant regulatory regions are required for *FT* transcription, reflecting the complexity of its control and differences in chromatin status delimit functionally important *cis*-regulatory regions.

INTRODUCTION

The transition to flowering is controlled by genetic pathways that integrate environmental cues and the developmental state of the plant. In *Arabidopsis thaliana*, several floral signals, including response to photoperiod, converge at the level of transcriptional regulation of the *FLOWERING LOCUS T* (*FT*) gene. Under inductive long-day (LD) conditions, the floral integrator *FT* is transcribed in the leaf vasculature (Takada and Goto, 2003; Notaguchi et al., 2008). Movement of FT protein is required to transport the LD signal to the meristem and initiate meristem identity changes (Abe et al., 2005; Wigge et al., 2005; Corbesier et al., 2007; Jaeger and Wigge, 2007; Mathieu et al., 2007). Misexpression of *FT* causes early flowering independent of environmental and endogenous stimuli, whereas loss of function of *FT* results in a severe late-flowering phenotype in LDs and has just a minor effect on flowering under noninductive short-day (SD) conditions (Koornneef et al., 1991; Kardailsky et al., 1999; Kobayashi et al., 1999).

FT belongs to a small protein family whose members show homology to mammalian phosphatidylethanolamine binding proteins, such as the Raf kinase inhibitor protein (Kardailsky et al., 1999; Kobayashi et al., 1999). The closest relative of *FT*, *TWIN SISTER OF FT* (*TSF*), produces a functionally equivalent protein but is expressed at much lower levels than *FT* (Michaels et al., 2005; Yamaguchi et al., 2005; Jang et al., 2009). By contrast, the related *TERMINAL FLOWER1* (*TFL1*) represses the floral transition and is expressed in the shoot apical meristem (Shannon and Meekswagner, 1991; Bradley et al., 1997). *FT/TSF* and *TFL1* define clearly separated spermatophyte-specific subfamiles that have further expanded in several species (Hedman et al., 2009).

Transcriptional activation of *FT* under inductive daylength conditions is directly mediated by CONSTANS (CO) (Samach et al., 2000). *CO* mRNA shows a circadian controlled pattern of accumulation in phloem companion cells, and CO protein is further stabilized by light, so that only in LD conditions does sufficient CO protein accumulate to induce *FT* (Suarez-Lopez et al., 2001; Valverde et al., 2004; Laubinger et al., 2006). *CO* encodes a nuclear protein containing two zinc binding B-boxes and a CCT (CONSTANS, CO-like, TIME OF CAB1) domain (Putterill et al., 1995; Robson et al., 2001). Direct binding of DNA by CO could not be demonstrated and led to the suggestion that CO requires partners to activate transcription (Suarez-Lopez et al., 2001). The CCT domain of CO is able to interact with components of the Nuclear Factor Y (NF-Y) complex (Ben-Naim et al., 2006; Wenkel et al., 2006). NF-Y proteins bind DNA as a heterotrimeric complex that recognizes *CCAAT cis*-elements (Mantovani, 1999; McNabb and Pinto, 2005). Genetic analysis demonstrated that members of the *A. thaliana* NF-Y complex are involved in flowering control and placed them in the photoperiodic pathway downstream of

[1] These authors contributed equally to this work.

[2] Address correspondence to turck@mpipz.mpg.de.

The author responsible for distribution of materials integral to the findings presented in this article in accordance with the policy described in the Instructions for Authors (www.plantcell.org) is: Franziska Turck (turck@mpipz.mpg.de).

[W] Online version contains Web-only data.

[OA] Open Access articles can be viewed online without a subscription.

www.plantcell.org/cgi/doi/10.1105/tpc.110.074682

CO (Cai et al., 2007; Chen et al., 2007; Kumimoto et al., 2008). Furthermore, it has been shown that the CO B-boxes interact with a member of the TGA family of basic domain/leucine zipper transcription factors (Song et al., 2008).

Several transcriptional repressors participate directly in *FT* regulation. The MADS box factors FLOWERING LOCUS C (FLC) and SHORT VEGETATIVE PHASE (SVP) form a complex that associates with regions within the proximal *FT* promoter and the first intron that comprise *CArG* boxes, although the importance of these elements for *FT* regulation has not yet been demonstrated (Searle et al., 2006; Li et al., 2008). In addition, members of two subfamilies of the AP2-related transcription factors physically interact with the *FT* locus and participate in transcriptional repression. *TEMPRANILLO1* (*TEM1*) and *TEM2* encode two partially redundant AP2-like proteins, and TEM1 binds to the *FT* 5′-untranslated region (Castillejo and Pelaz, 2008). *SCHLAFMÜTZE* (*SMZ*) belongs to a subclade of the AP2 family that is targeted by *miR172* (Aukerman and Sakai, 2003). Overexpression of *SMZ* but also of other members of the subclade strongly represses *FT*, whereas overexpression of *miR172* accelerates the transition to flowering in a partially *FT*-dependent manner. SMZ binding sites have been identified at the genomic level, and, surprisingly, SMZ binds several kilobases downstream of the *FT* coding sequence (Mathieu et al., 2009).

Chromatin-associated protein complexes add another layer of complexity to *FT* regulation (Farrona et al., 2008; Del Olmo et al., 2009; Jeong et al., 2009). Loss of function of *LIKE HETEROCHROMATIN PROTEIN1* (*LHP1*), also known as *TFL2*, causes daylength-independent early flowering mainly due to upregulation of *FT* expression (Kotake et al., 2003). *LHP1* is expressed in meristematic tissues and young leaves, whereas expression in developing leaves becomes restricted to the petiole and the proximal side of the leaf blade, areas where cells continue to proliferate. In mature leaves, *LHP1* mRNA is restricted to the vascular tissue (Kotake et al., 2003). *LHP1* is a single-copy gene that encodes a protein containing a chromo domain and a chromo shadow domain. Chromo domains bind Lys-methylated proteins and have been identified in many chromatin-associated proteins, while the chromo shadow domain is a distinctive feature of the animal HETEROCHROMATIN PROTEIN1 (HP1) family. Whereas the best known member of the HP1 family is predominantly involved in the stabilization of constitutive heterochromatin, the plant homolog LHP1 is dedicated to transcriptional regulation of genes located in the euchromatin (Nakahigashi et al., 2005). Through its chromodomain, LHP1 colocalizes exclusively and extensively with genes that also possess nucleosomes with trimethylated Lys residues at position 27 of histone 3 (H3K27me3) (Turck et al., 2007; Zhang et al., 2007a; Exner et al., 2009).

Trimethylation of H3K27 is performed by the Polycomb repressive complex 2 (PRC2) that is conserved between plants and animals (Farrona et al., 2008; Schatlowski et al., 2008; Luo et al., 2009). In animals, H3K27me3 is bound by the chromo domain of the Polycomb (Pc) protein, a subunit of PRC1 (Schuettengruber et al., 2007). The idea that LHP1 may be part of a plant PRC1 and fulfill a function analogous to Pc is supported by recent results showing that LHP1 can interact with RING1A, the homolog of the animal PRC1 core component Sex Combs Extra (Xu and Shen, 2008). LHP1 and H3K27me3 histone marks distribute widely over the *FT* locus, indicating that this gene is regulated by the Polycomb Group (PcG) pathway (Turck et al., 2007; Zhang et al., 2007b). The early flowering, high *FT* expressing phenotype of several mutants in PRC2 encoding genes further corroborates this conclusion (Farrona et al., 2008).

Previous studies have demonstrated the importance of transcriptional regulation of *FT* to ensure flowering time control in response to environmental and endogenous factors. Several transcription factors and chromatin-associated proteins have been shown to target different regions within the *FT* locus, but so far the relevance of the targeted regions for *FT* regulation has not been firmly established. Here, we show that CO-dependent *FT* activation requires not only proximal but also conserved distal promoter regions that together with LHP1-mediated chromatin status orchestrate the interplay between activating and repressing inputs to FT regulation.

RESULTS

Identification of Putative *FT* Regulatory Sequences by Phylogenetic Shadowing

To identify candidate sequences for regulatory motifs, we aligned sequences from 7.0 kb upstream of *FT* from *A. thaliana* accession Columbia (Col) (Figure 1A) to *FT* sequence from *A. thaliana* accession Landsberg *erecta* (L*er*) and *FT* homologous genes from *Arabidopsis lyrata*, *Brassica rapa*, and *Arabis alpina* (Aa *FT1*-Aa *FT3*). The pairwise alignment revealed three highly conserved sequence blocks (Figure 1B, highlighted in light gray). *Block A*, closest to the *FT* start codon, showed high conservation among *A. thaliana*, *B. rapa*, and Aa *FT1*. Expanding the alignment with homologous sequences of *Sisymbrium polyceratum*, *Brassica oleracea*, *Capsella rubella*, and *Arabis hirsuta* revealed highly conserved sequence stretches within *block A* of the Aa *FT2* and Aa *FT3* genes and in the promoter sequence of *A. thaliana TSF* (Figure 1C). These putative *cis*-regulatory elements did not contain documented transcription factor binding sites and were therefore called *shadow 1*, *2*, *3*, and *4* (*S1* to *S4*). Furthermore, two palindromic sequences flanking *S3* were identified and named *P1* and *P2*. *Block B* is located around 1.8 kb upstream of *FT* and contains two highly conserved sequence stretches that include an E-box, which is a binding site for many basic-helix-loop-helix (bHLH) proteins like Cryptochrome-interacting bHLH 1 (CIB1), which has been shown to enhance *FT* expression in response to blue light (Liu et al., 2008; Figure 1D). A third conserved *block C*, located around 5.2 kb upstream of the *FT* start codon, is identified by the alignment of *FT* promoter sequences of the *Arabidopsis* genus and *B. rapa* (Figure 1B) and is conserved in *C. rubella* (Figure 1E). Prediction of transcription factor binding sites revealed a conserved *CCAAT* box, the binding site for the NF-Y complex (Mantovani, 1999). Furthermore, a *GATAA* motif, called I-box, present in many light-regulated genes in monocots and dicots (Terzaghi and Cashmore, 1995), is conserved in *block C*, as well as an REalpha consensus sequence (*AACCAA*) that has been implicated in regulation by phytochromes (Degenhardt and Tobin, 1996).

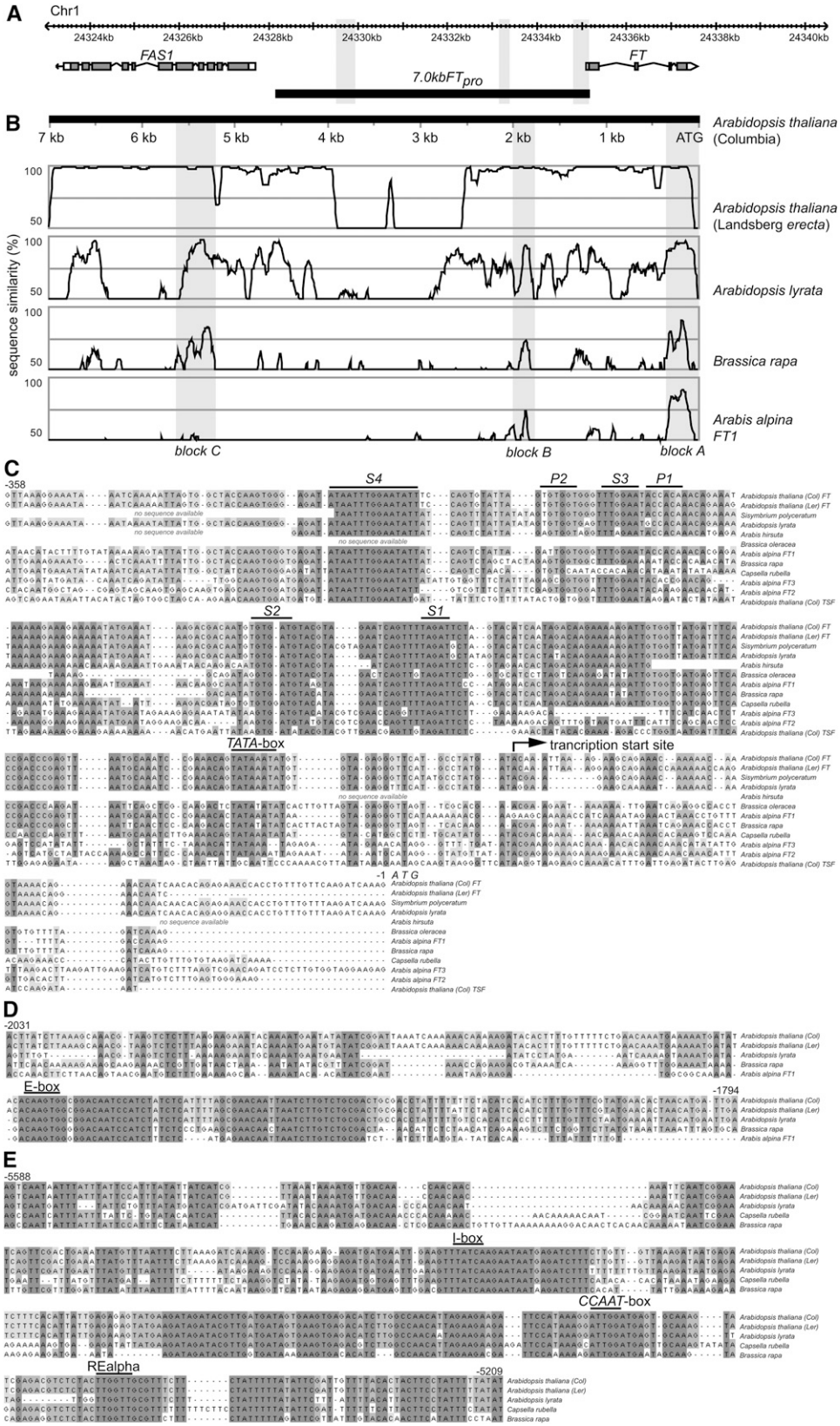

Figure 1. Conservation of *FT* Promoter Sequences.

The 5.7-kb Sequence Upstream of the *FT* Translation Start Site Contains Sufficient Regulatory Information to Mediate to Daylength Response in Col

Previously, it has been shown that a transgene consisting of 8.9-kb sequence upstream of the *FT* translation start site fused to the cDNA of *FT* complements the *ft-1* late flowering phenotype (Takada and Goto, 2003). To further delimit the upstream regulatory region of *FT*, a set of deletion constructs was generated (Figure 2A). Complementation analysis of deletion constructs between 8.1 and 4.0 kb in length revealed that 5.7-kb sequence upstream of *FT* fused to the *FT* cDNA (Figure 2A) was sufficient to rescue the late flowering phenotype of *ft-10* plants grown under inductive extended short-day (ESD) conditions (Figure 2B). Under noninductive SD conditions, transgenic complementation lines containing *FT* promoter fragments of 5.7 kb and longer mimicked the flowering behavior of wild-type plants, as shown for the longest fragment in Supplemental Figure 1A online. β-Glucuronidase (*GUS*) expression driven by a *FT* promoter fragment of 5.7 kb was restricted to the vasculature of cotyledons and the minor veins of the distal half of the leaf as had been previously reported for longer *FT* promoter fragments (Takada and Goto, 2003) (Figure 2C). GUS signal was not detected in shoot apical regions, hypocotyls, or roots and was almost absent in plants grown under SD conditions. Even the strongest expressing *8.1kbFT$_{pro}$:GUS* line showed only single stained cells in the vasculature of some leaves in SDs (see Supplemental Figure 1B online, magnification). Quantification of *GUS* and *FT* mRNA levels with absolute standards showed that the transgene closely follows the expression of the endogenous gene under different conditions (see Supplemental Figure 1C online).

Published data on the spatial *FT* expression pattern in plants ubiquitously expressing *CO* are contradictory. While Takada and Goto (2003) showed that ectopic *CO* expression led to ubiquitous GUS signal, the same *8.9kbFT$_{pro}$:GUS* transgene when studied by the Araki group revealed *GUS* expression that was restricted to the vasculature in spite of ubiquitous *CO* expression (Yamaguchi et al., 2005). In our hands, expression of the *GUS* reporter gene under control of 5.7 kb or longer *FT* promoter fragments was extended in *35S$_{pro}$:CO* plants to all major veins of the leaves but not beyond (Figure 2C).

Shortening the *FT* promoter to 4.0 kb upstream of the translation start site (Figure 2A) disrupted its ability to drive *FT* cDNA expression and therefore to complement the *ft-10* mutant phenotype (Figure 2B). Likewise, *4.0kbFT$_{pro}$:GUS* Col plants grown for 10 d in ESD showed no GUS signal (Figure 2C). In older seedlings carrying the same transgene, *GUS* expression was detectable in the Y junction of the hypocotyl vasculature close to the meristem (see Supplemental Figure 2 online), but expression in a few hypocotyl cells below the meristem was not sufficient to trigger flowering if the 4.0-kb promoter was used to drive *FT* cDNA expression (Figure 2B). Furthermore, expression of the *GUS* reporter gene under control of a 4.0-kb *FT* promoter was not induced in *35S$_{pro}$:CO* seedlings (Figure 2C). In flowering *4.0kbFT$_{pro}$:GUS* Col plants, GUS signal showed at the base of carpels and siliques and along the septum, which suggests that the *4.0kbFT$_{pro}$:GUS* construct is functional (see Supplemental Figure 2 online). No GUS signal showed in wild-type seedlings carrying a *GUS* reporter gene under control of a proximal 1.0 kb (−1000 to −1) *FT* promoter (Figure 2C), but during flower development, *GUS* expression became visible in pollen (see Supplemental Figure 2 online). In *1.0kbFT$_{pro}$:GUS 35S$_{pro}$:CO* seedlings, GUS signal was only observed in single phloem cells of the leaf (Figure 2C), at the base of leaf trichomes and a few mesophyll cells in hypocotyls.

In summary, *FT* promoter sequence 5.7 kb upstream of the translation start site contains all regulatory elements required to mediate spatial and temporal expression of *FT* in response to photoperiod. Since shortening of the promoter to 4.0 kb abolished the ability to mediate daylength-dependent activation, a distal promoter region containing the conserved *block C* seems to comprise important regulatory sequences. A 4.0-kb *FT* promoter is not responsive to high CO levels, whereas a 1.0-kb *FT* promoter is marginally induced.

Identification of *cis*-Acting Elements in the Proximal *FT* Promoter

Residual expression driven by a 1.0-kb *FT* promoter together with high conservation of *block A* indicates a regulatory function of the proximal sequence. Surprisingly, in transient expression

Figure 1. (continued).

(A) Genome browser view of the *FT* locus on chromosome 1 in *A. thaliana* accession Col. Exons of *FT* and the flanking gene *FAS1* are represented as gray boxes and untranslated regions as white boxes. Arrows indicate the direction of transcription. The promoter sequence used for pairwise alignment is represented by a black box. Light-gray areas highlight the conserved regions *block A*, *block B*, and *block C*.

(B) Pairwise alignment of *FT* promoter sequences from different species to 7.0-kb *FT* promoter sequence of *A. thaliana* Col using mVISTA (see Supplemental Data Sets 1 to 4 online). Graphical output shows basepair identity in a sliding window of 75 bp in a range of 50 to 100%. Light-gray areas highlight conserved blocks that were further analyzed with ClustalW2. Several other minor peaks observed with mVISTA were caused by general AT richness of the underlying sequence.

(C) Sequence alignment of the proximal *FT* promoter (−1 to −358 bp, *block A*). Four conserved sequence stretches were identified and called *shadow 1* to *4* (*S1* to *S4*). A palindromic sequence flanking *S3* is labeled as *P1* and *P2*. Furthermore, the putative *TATA* box and the transcription start site are indicated.

(D) Alignment of a region with high conservation (−1794 to −2031 bp), named *block B*. *Block B* shows two highly conserved sequence stretches, and a conserved E-box is indicated.

(E) Sequence alignment of a distal *FT* promoter region (−5209 to −5588 bp), named *block C*. Predicted conserved *CCAAT*-box, a *GATAA* motif, called I-box, and a REalpha consensus sequence (*AACCAA*) are indicated.

Multiple alignments were obtained with ClustalW2 (see Supplemental Data Set 5 online). Intensity of the shading corresponds to the degree of conservation.

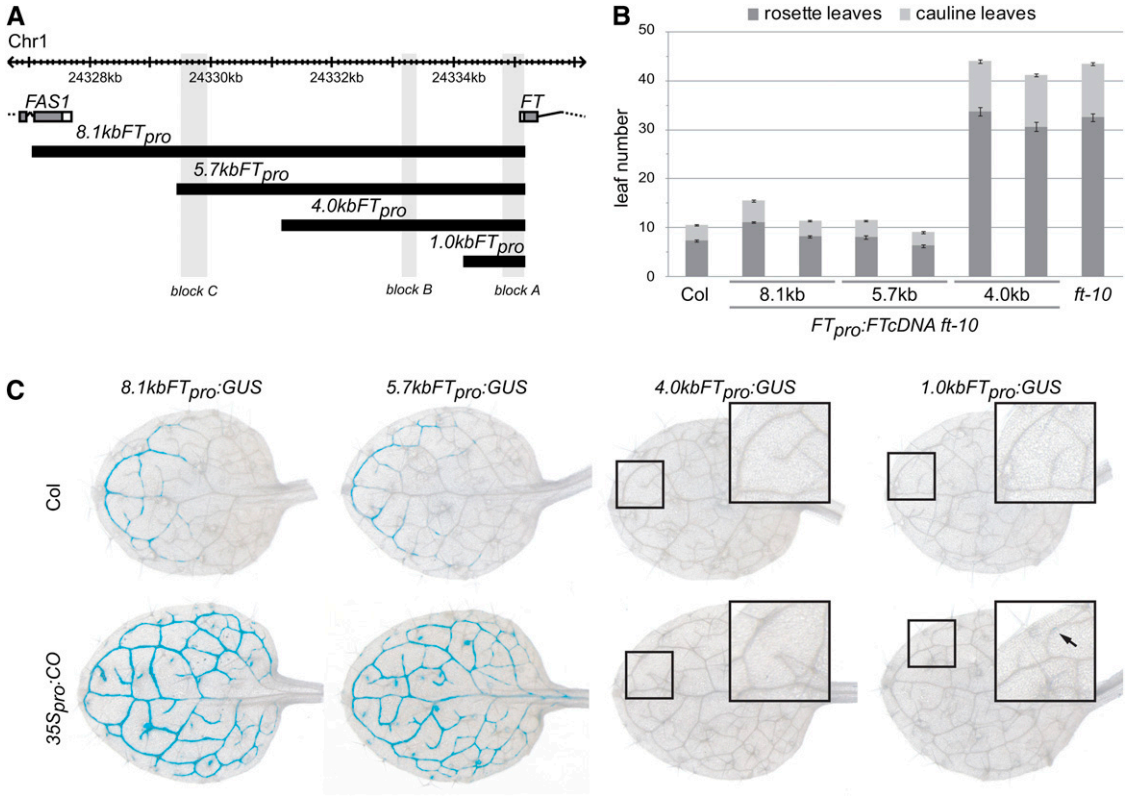

Figure 2. CO-Mediated Induction of *FT* Requires Sequences between 4.0 and 5.7 kb Upstream of the *FT* Gene.

(A) Genome browser view of the *FT* upstream sequences. Promoter constructs used for analyses are depicted as black boxes.
(B) Flowering time of *ft-10* plants carrying transgenic constructs driving *FT* cDNA by an 8.1-, 5.7-, and 4.0-kb *FT* promoter fragment. Two independent transgenic lines are shown for each construct; wild-type plants and *ft-10* mutants were analyzed as control. Plants were grown under inductive ESD conditions. The experiment was repeated twice with similar results. Number of rosette and cauline leaves of a representative example are shown as the mean ± SE.
(C) Histochemical localization of GUS activity in first true leaves of *8.1kbFT$_{pro}$:GUS*, *5.7kbFT$_{pro}$:GUS*, *4.0kbFT$_{pro}$:GUS*, and *1.0kbFT$_{pro}$:GUS* plants. Transgenic plants in Col and *35S$_{pro}$:CO* background were grown for 10 LDs on soil. Insets show a higher magnification of an area of the distal half of the leaves. Arrow indicates a single GUS-stained phloem cell.

studies performed by leaf bombardment, constructs with a luciferase gene under control of an 8.1-, 4.0-, or 1.0-kb *FT* promoter fragment showed no difference in expression. Cobombardment with *35S$_{pro}$:CO* increased the luciferase signal from all constructs around sixfold (Figure 3A). Reporter constructs with point mutations in *block A* elements were therefore tested in the context of the 1.0-kb *FT* promoter in transient assays (Figure 3B). Compared with the original sequence, mutations in *S2* and in the two palindromic sequences *P1/P2* reduced luciferase activity in response to CO by twofold. Presence of *S3* had only a slight impact on CO-mediated stimulation, while mutations in *S1* did not affect luciferase activity.

To study the biological relevance of *S2*, *S3*, and *P1/P2* in the genomic context, mutations in these elements were introduced into the 8.1-kb *FT* promoter fragment and analyzed in complementation experiments using stable transformation of *ft-10* plants (Figure 3C). Among 10 lines tested, seven *8.1kbFT$_{pro}$-S2mut:FTcDNA ft-10* lines flowered significantly later than the *8.1kbFT$_{pro}$:FTcDNA ft-10* control. The *8.1kbFT$_{pro}$-S3mut:FTcDNA ft-10* plants flowered with a similar number of leaves as plants containing the nonmutated construct. Mutation of the palindromic sequence *P1/P2* had a strong impact on expression since *8.1kbFT$_{pro}$-P1/P2mut:FTcDNA ft-10* lines did not complement the late flowering phenotype. Flowering time data were well correlated with transcript levels generated by the transgenes (Figure 3D).

Taken together, two phylogenetically conserved sequences within the proximal promoter have been identified that act as positive *cis*-elements in *FT* regulation.

LHP1-Mediated Repression of *FT* through a Regulatory Element Located between 1.0 and 4.0 kb Upstream of *FT*

The spatial expression pattern driven by *FT* promoter fragments of different length was analyzed in the *lhp1* background (Figure 4). As already reported for a slightly longer construct (Takada and Goto, 2003), the expression pattern of *8.1kbFT$_{pro}$:GUS* in *lhp1* mutants was extended to the middle vein as well to minor veins of

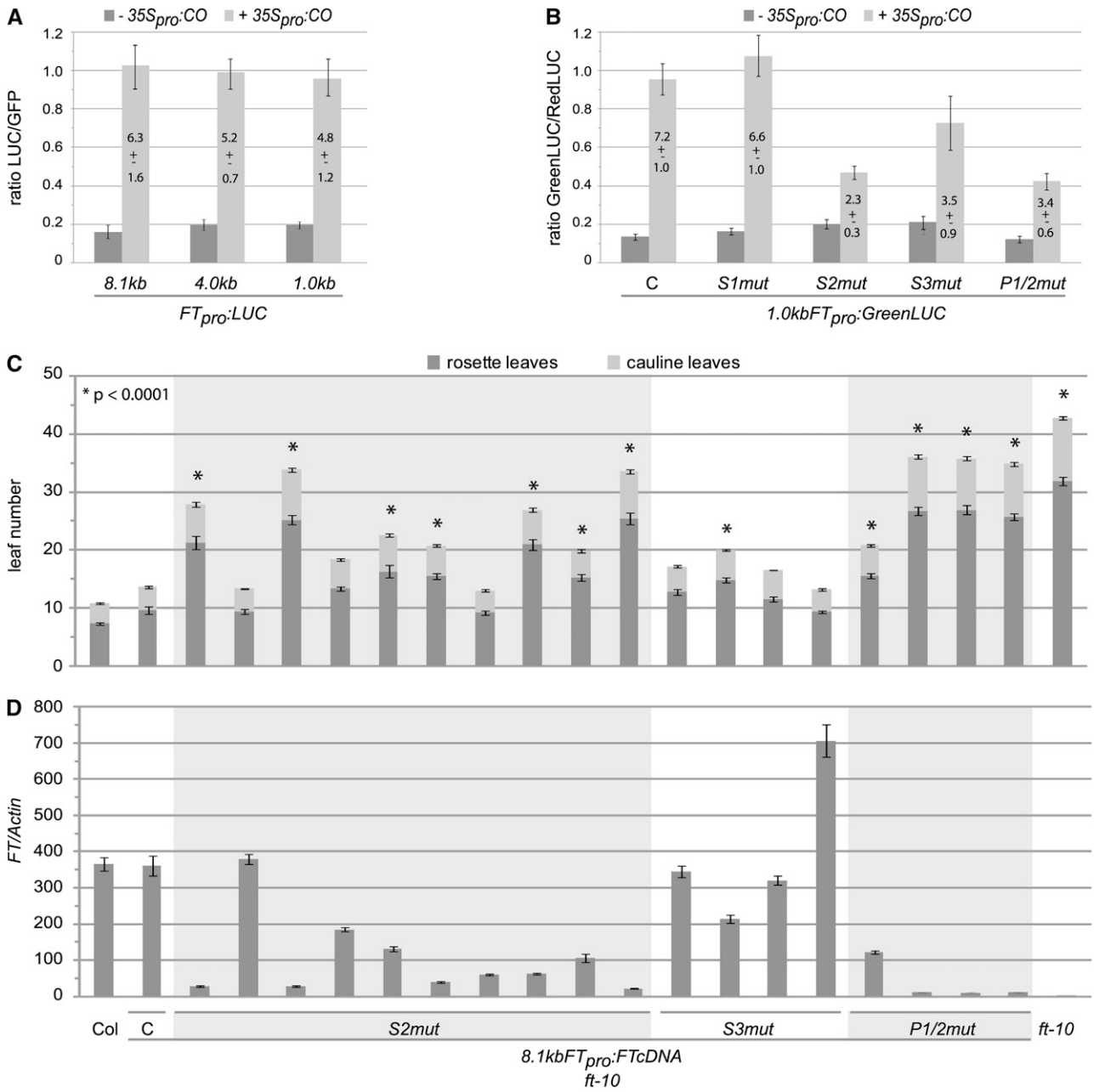

Figure 3. Proximal *FT* Promoter Sequences Are Crucial for Mediating Daylength Response.

(A) A transient expression assay was performed using a luciferase gene (*LUC*) under control of *FT* promoter fragments of 8.1, 4.0, and 1.0 kb in length. CO-dependent transcriptional activation was analyzed by cobombardment of $35S_{pro}$*:CO*. Light emission per leaf was normalized to the fluorescence signal obtained from a cobombardment of the $35S_{pro}$*:GFP* construct. Fold stimulation of the promoter by CO is indicated within the light-gray bar for each construct. Data from three independent experiments are shown as mean ± SE.

(B) The $1.0kbFT_{pro}$*:GreenLUC* constructs carrying mutations in different putative *cis*-elements of the promoter were tested in a transient expression assay. Resulting green light emission was normalized to light emission of a cobombarded red light emitting luciferase (RedLUC). CO-dependent transcriptional activation was analyzed by cobombardment of $35S_{pro}$*:CO*. Fold stimulation of the promoter by CO is indicated within the light-gray bar for each construct. Mean ± SE is based on at least three independent experiments.

(C) Flowering time of *ft-10* plants carrying transgenic constructs driving *FT* cDNA by mutated versions of the 8.1-kb *FT* promoter fragment. Several independent transformants are shown for each construct; wild-type plants, $8.1kbFT_{pro}$*:FTcDNA ft-10* carrying no mutation (labeled as C in the graph), and *ft-10* mutants were analyzed as controls. Plants were grown in ESD conditions. The experiment was repeated two times with similar results. Differences in total leaf number compared with $8.1kbFT_{pro}$*:FTcDNA ft-10* plants were analyzed with a two-way analysis of variance. Asterisks indicate significant differences with P values < 0.0001. Number of rosette and cauline leaves of a representative experiment are shown as the mean ± SE.

the proximal part of the first true leaves (Figure 4). Interestingly, the 4.0-kb *FT* promoter fragment that was not able to drive expression in either wild-type or *35S$_{pro}$:CO* plants became active in *lhp1* seedlings. GUS signal was observed in the major vein and the proximal vascular tissue in leaves of *4.0kbFT$_{pro}$:GUS lhp1* plants. Although transgenic *1.0kbFT$_{pro}$:GUS* Col plants did not show expression when grown on soil (Figure 2B), seedlings grown on agar occasionally showed *GUS* expression in single phloem cells of the distal leaf vasculature (Figure 4, magnification). In the *lhp1* mutant background, *GUS* expression driven by a 1.0-kb *FT* promoter was detectable in all transgenic lines, although the observed pattern differed. Most lines showed GUS signal in the tip and the hydathodes of leaves (Figure 4) and the Y junction of the vasculature close to the meristem. One *1.0kbFT$_{pro}$:GUS lhp1* line showed additional GUS signal in the distal minor veins of leaves (Figure 4) and in the entire vasculature of the hypocotyl. Among five lines tested, a single *1.0kbFT$_{pro}$:GUS lhp1* line showed GUS activity in the vasculature of roots, hypocotyls, and petioles and in the middle vein of the basal part of leaves. The differing GUS pattern among these lines could be explained by differences in the genomic context, indicating that this promoter fragment alone does not induce expression but depends on the recruitment of adjacent regulatory sequences.

In summary, LHP1 mediates repression of *FT* in the middle vein by neutralizing an enhancer element located between 1.0 and 4.0 kb upstream of the start codon. Furthermore, expression driven by a 1.0-kb proximal promoter fragment was enhanced in the *lhp1* mutant but probably also dependent on the recruitment of additional regulatory elements.

FT Chromatin Changes Correlate with Its Transcriptional State

To investigate how transcriptional activation of *FT* by CO is reflected by changes in the chromatin, chromatin immunoprecipitation (ChIP) experiments were performed with chromatin obtained from *35S$_{pro}$:LHP1:HA* and *35S$_{pro}$:LHP1:HA 35S$_{pro}$:CO* seedlings. Since binding of LHP1 has been shown to colocalize with the H3K27me3 histone mark (Turck et al., 2007; Zhang et al., 2007a), occurrence of LHP1:HA and H3K27me3 were analyzed along the *FT* locus (Figure 5A). Plants were grown in SDs so that only *35S$_{pro}$:CO* seedlings expressed *FT*. In these plants, LHP1:HA binding was reduced along the *FT* structural gene and the proximal promoter compared with nonexpressing wild-type background (Figure 5B). By contrast, signal strength for the H3K27me3 histone mark did not significantly differ along the *FT* locus in seedlings differentially expressing *FT* (Figure 5C).

Histone acetylation of regulatory regions often positively correlates with gene expression either because transcription factors act through the recruitment of histone acetyl-transferases or because of histone acetyl-transferase activity that is recruited during the transcriptional process (Choi and Howe, 2009). ChIP experiments were performed with an antibody that detected acetylation of H3K9 and K14 (H3K9K14ac). Indeed, acetylation of H3 was increased in the proximal promoter and the transcribed region of *FT* in *35S$_{pro}$:CO* plants (Figure 5D). Furthermore, H3K9K14ac increased in a distal *FT* promoter region that overlapped with the conserved *block C*. Acetylation at the distal region could be due to transcriptional upregulation of the closely located *FASCIATA1* (*FAS1*) gene, but levels of *FAS1* are not altered in *35S$_{pro}$:CO* plants (see Supplemental Figure 3 online). Therefore, increased H3K9K14ac levels are likely to be linked to *FT* expression changes.

Taken together, expression of *FT* correlates with a depletion of LHP1 from *FT* without a corresponding change in the H3K27me3 modification pattern. In plants actively transcribing *FT*, H3K9K14ac was increased in distal and proximal regulatory regions and at the structural gene.

Analysis of Changes of *FT* Chromatin Immediately upon Transcriptional Activation

Use of plants constitutively overexpressing *CO* cannot distinguish between chromatin changes being the cause or consequence of *FT* expression. Therefore, we introduced the *35S$_{pro}$:LHP1:HA* reporter into a *35S$_{pro}$:CO:GR* line. Treatment of these plants with dexamethasone (Dex) causes nuclear import of cytosolic CO:GR fusion protein within 15 min (see Supplemental Figure 4A online) and leads to a steep increase in *FT* expression after a lag phase of 1 h and 30 min and flowering (Figure 6A; see Supplemental Figure 4B online). Samples for ChIP experiments were taken every 30 min for up to 3 h after Dex treatment. As expected, H3K27me3 levels at the *FT* locus did not change during the induction (Figure 6C). LHP1:HA was only slightly reduced at the proximal promoter and the structural gene at the later time points when *FT* expression was already significantly increased (Figure 6B). Furthermore, no changes in acetylation levels that anticipated the increase in expression of *FT* could be observed at the proximal and distal regulatory regions (Figure 6D).

In conclusion, decrease in LHP1 binding and increased acetylation of H3K9K14 at *FT* that were observed in plants expressing the *FT* activator CO constitutively seem to be a consequence of prolonged *FT* transcription but are not a prerequisite for early *FT* activation.

High-Resolution Mapping of H3K27me3 and LHP1:HA at *FT* Identifies a Locally Depleted Region

Recruitment of LHP1-associated repressive complexes by H3K27me3 are believed to lead to a more condensed chromatin state that is inaccessible for *cis*-regulatory element binding

Figure 3. (continued).

(D) Quantitative PCR of *FT* expression in *ft-10* seedlings carrying nonmutated and mutated versions of the *8.1kbFT$_{pro}$:FTcDNA* transgene. Plant material was harvested at ZT 16 on day 10 under ESD conditions. Molarity of mRNA (pmol) was calculated and normalized by *Actin* (pmol). Error bars represent SE of the mean based on three technical replicates.

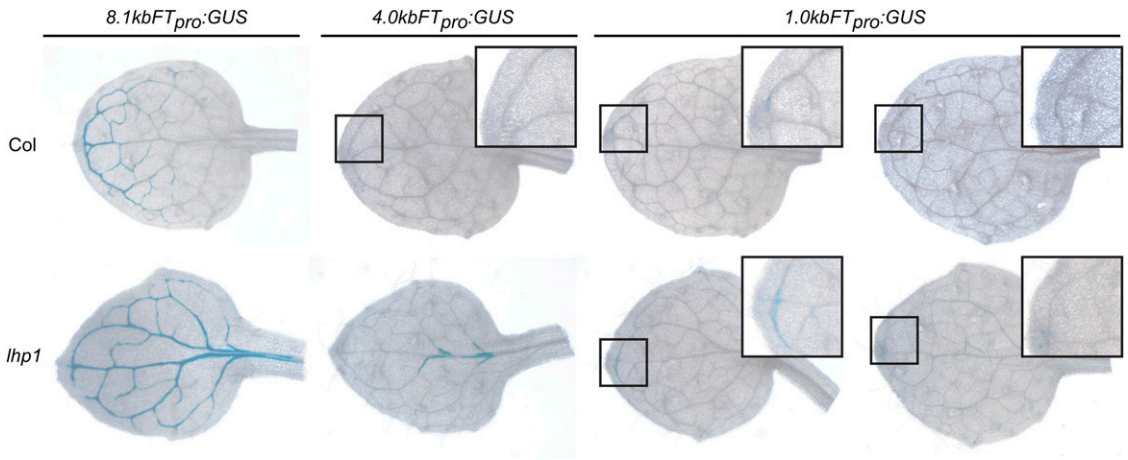

Figure 4. LHP1 Mediates *FT* Transcriptional Regulation through 4.0-kb *FT* Promoter Region.

Spatial *GUS* expression pattern in first true leaves of *8.1kbFT$_{pro}$:GUS*, *4.0kbFT$_{pro}$:GUS*, and *1.0kbFT$_{pro}$:GUS* plants grown for 10 LDs on agar. Transgenic plants in Col and *lhp1* background are based on independent transformations. Insets show a higher magnification of an area of the distal half of the leaves.

transcription factors (Farrona et al., 2008). Since *FT* transcriptional activation does not require the prior removal of the chromatin-mediated repressor, other mechanisms must be in place to allow transcriptional activator access to *FT*. High-resolution mapping of the chromatin at the *FT* locus by ChIP-chip experiments with high-density microarrays revealed that the conserved *block C* coincides with a locally H3K27me3 and LHP1 poor region (Figure 7A; see Supplemental Data Set 6 online). In addition, the proximal promoter was partially depleted in both repressive chromatin marks.

DISCUSSION

FT Promoter Comprises a Complete Set of *FT* Regulatory Elements

Previous studies analyzed spatial expression of a *GUS* reporter gene under control of an 8.9-kb *FT* promoter or integrated into a genomic fragment covering 7.2 kb upstream and 1.5 kb downstream of *FT* and found that these did not differ in their expression patterns (Notaguchi et al., 2008). These data supported the idea that CO-responsive elements are located upstream of *FT*. Our data demonstrate that an 8.1-kb *FT* promoter also drives expression in the same temporal pattern and quantitative range as the endogenous *FT* gene, under inductive and noninductive conditions (Figure 2; see Supplemental Figure 1C online). This result is somewhat surprising as a regulatory role has been postulated for the first intron of *FT*, which encompasses a *CArG* box as putative binding site for the interacting transcriptional repressors FLC and SVP (Searle et al., 2006; Li et al., 2008). However, a *CArG* box as binding site for SVP has also been identified in the proximal *FT* promoter, and so it is plausible that the two *CArG* boxes are redundant in summer annual *A. thaliana* plants expressing low levels of *FLC*.

As shown in this (Figure 2) and a previous study (Notaguchi et al., 2008) *FT* expression is restricted to the vasculature despite a ubiquitous ectopic expression of *CO*. CO activity is dependent on the stabilization of the protein by light perceived at the end of long days (Valverde et al., 2004; Turck et al., 2008), and a lack of CO accumulation in other tissues could explain the phloem-specific expression pattern of *FT* in *35S$_{pro}$:CO.* However, analysis of plants expressing a *35S$_{pro}$:CO:GFP* fusion in *A. thaliana* demonstrated that CO protein is stable outside of the vasculature, as green fluorescent protein (GFP) signal was detectable in nuclei of epidermal cells (Valverde et al., 2004). Hence, the observations support the idea that CO requires an unidentified protein partner or complex to activate transcription and suggest that at least one factor of this CO activator complex is specific to the vasculature.

Our data show that 5.7-kb sequence upstream of the translation start site of *FT* encodes sufficient *cis*-regulatory elements to mediate tissue-specific and CO-responsive expression, whereas shortening the *FT* promoter to 4.0 kb upstream of the *ATG* disrupts the ability of CO to drive *FT* expression (Figure 2). Therefore, sequences between 4.0 and 5.7 kb upstream of *FT ATG* seem to contain crucial regulatory elements required for the response to CO. A phylogenetic shadowing approach identified a conserved region (*block C*) located around 5.2 kb upstream of *FT* (Figures 1B and 1E). Sequence conservation of regulatory regions is likely to reflect the constraint to maintain gene regulation during evolution. The underlying model is that mutations have been counterselected in sites recognized by transcription factors, thereby imposing a slower rate of divergence than in surrounding sequences (Vavouri and Elgar, 2005). Notably, the evolutionary conserved regions *block C* and *block B* included two putative *cis*-regulatory elements that are recognized by transcription factors with a suggested role in *FT* regulation (Ben-Naim et al., 2006; Wenkel et al., 2006; Liu et al., 2008).

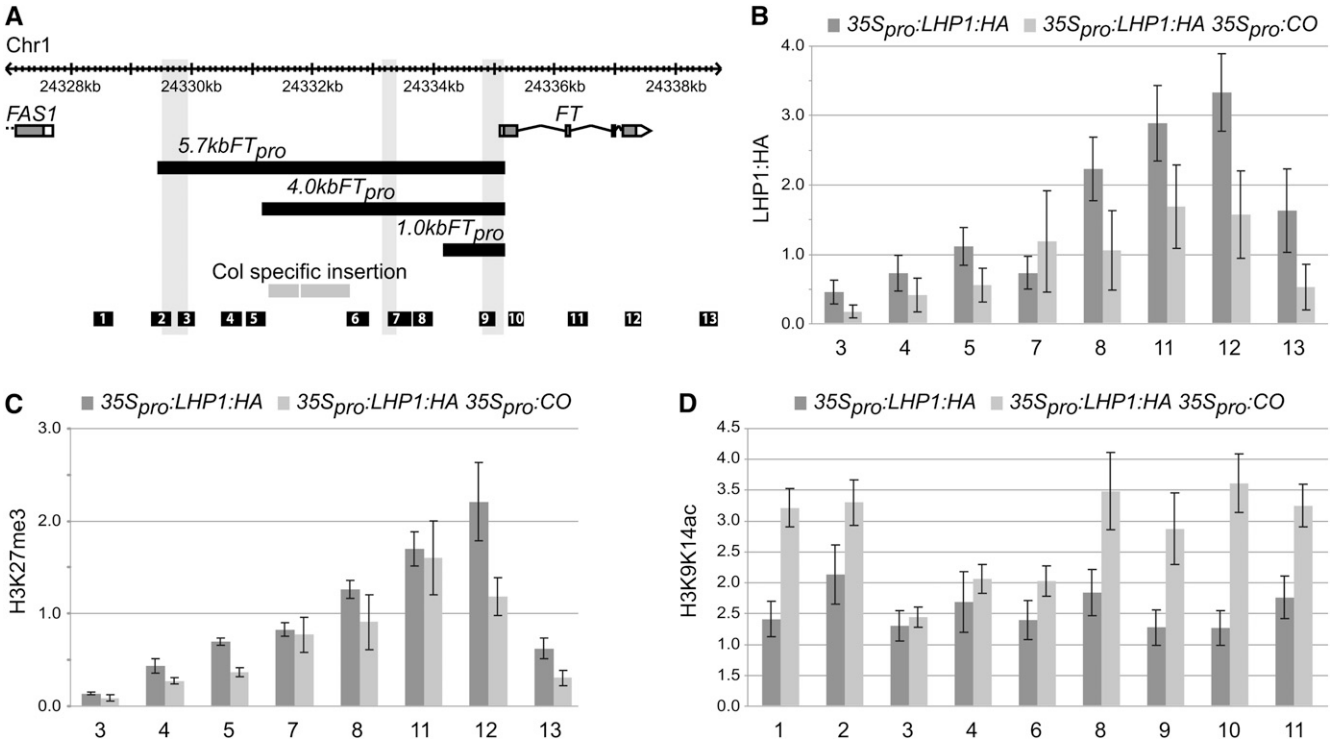

Figure 5. Chromatin Changes in Highly *FT* Transcribed Conditions.

(A) Genome browser view of the *FT* locus as shown before. Two Col-specific insertions that are not present in L*er* are depicted in gray. Positions of amplicons used in the ChIP analysis are presented as black boxes and are numbered.

(B) Binding of LHP1 at the *FT* locus. ChIP experiments were performed with chromatin from $35S_{pro}$*:LHP1:HA* and $35S_{pro}$*:LHP1:HA* $35S_{pro}$*:CO* L*er* plants grown for 10 d under SD conditions. Signals detected along the *FT* locus were normalized with the signal obtained for *At4g24640*, which is not under the regulation of CO but is a LHP1 target.

(C) Trimethylation of H3K27 at *FT* in $35S_{pro}$*:CO* plants. Data are based on the same chromatin extract and analysis as used in **(B)**.

(D) Acetylation of H3K9 and K14 in the promoter and the transcribed region of *FT* in seedlings ubiquitously expressing *CO*. The experiment is based on the same chromatin extract as used in **(B)**. Data were normalized using the highly transcribed *At1g67090*.

Data in **(B)** to **(D)** are shown as the mean of a representative experiment. Error bars show the 95% confidence interval of three technical replicates.

The phylogenetic shadowing approach further identified a promoter region just upstream of the *FT* transcription start site (*block A*, Figure 1B) that is highly conserved between different *Brassicacea* plants (Figure 1C). Complementation and expression analysis confirmed the relevance of shadow *S2*, whose mutation results in reduced *FT* expression, and of the palindromic sequence *P1/P2*, apparently essential for *FT* expression (Figures 3C and 3D). So far, there are no candidate transcription factors that recognize the DNA sequences *S2* and *P1/P2*.

Although histochemical *GUS* localization assays showed that a 1.0-kb *FT* promoter alone was barely able to drive expression in Col, this residual expression was enhanced under highly inductive conditions (Figures 2 and 4). Moreover, in transient expression assays, the proximal 1.0-kb *FT* promoter was inducible by CO. We propose a model where CO acts through the proximal promoter but requires interaction with an activator complex that associates with the distal regions of the *FT* promoter (Figure 7B). Interaction with a protein partner could enhance affinity of CO to DNA and thereby lead to binding of the proximal promoter region. In transient assays, extremely high amounts of DNA are introduced into bombarded cells, and interaction with a coactivator might not be required. On the other hand, expression driven by a 1.0-kb *FT* promoter in the transient reporter assay may well be due to general differences between bombarded and integrated DNA. While the transgene is integrated into the genomic context in stably transformed plants, genes encoded on plasmids lack certain aspects of regulation mediated through chromatin (Hebbar and Archer, 2007). Therefore, the role of factors binding to the distal region could be to increase the accessibility of the proximal region, an action not required if the controlled region is already accessible.

Chromatin Changes at *FT* Play a Permissive Role

It has been proposed that LHP1 counteracts the activity of CO on *FT* to ensure daylength-dependent flowering (Takada and Goto, 2003). As *CO* and *LHP1* are expressed in an inverted gradient along the leaf, *FT* transcription in the distal veins was proposed to occur as a result of CO overcoming the repressive effect of decreasingly expressed *LHP1*. Introducing *FT* promoter deletion

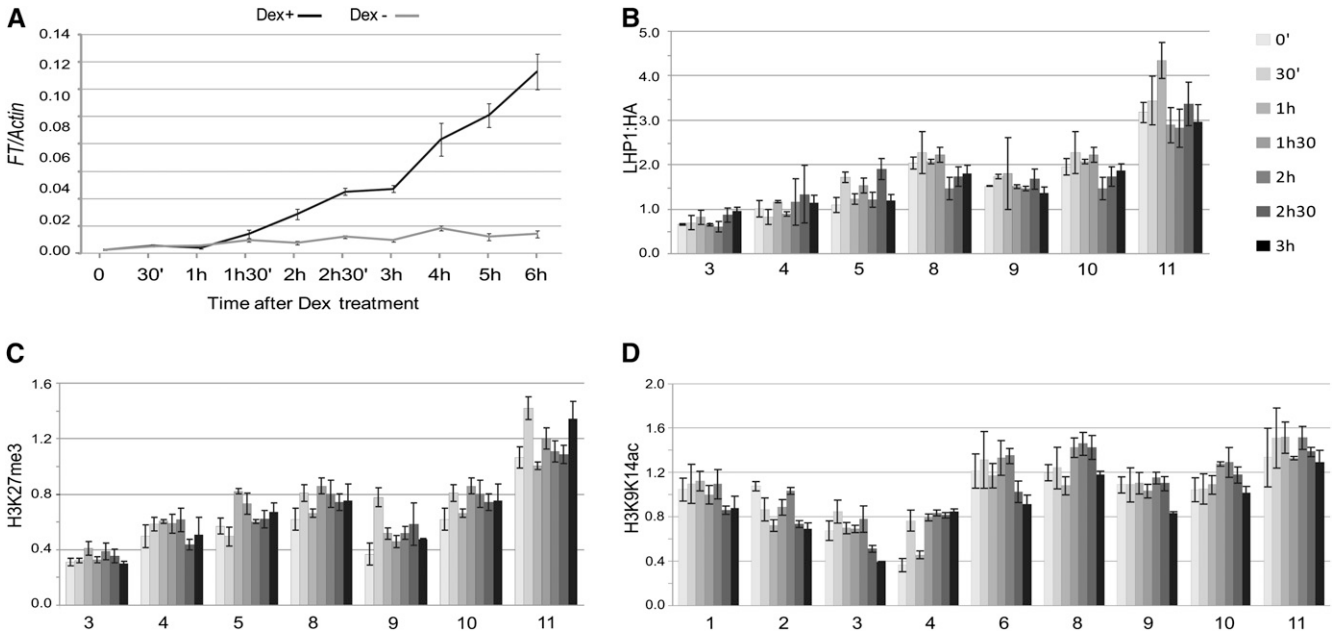

Figure 6. Chromatin Changes at the *FT* Locus upon Early *FT* Induction.

(A) Temporal *FT* expression upon CO induction. *35S$_{pro}$:LHP1:HA 35S$_{pro}$:CO:GR* L*er* seedlings were grown under noninductive SD conditions. At day 10, plant material was harvested every 30 min after Dex (Dex+) or mock (Dex−) treatment. Expression levels of *FT* mRNA were normalized by *Actin*. Data are shown as the mean of a representative experiment. Data are based on three technical replicates. Error bars show the SD of three technical replicates.
(B) Binding pattern of LHP1 to the *FT* locus upon induction of *FT* transcription. ChIP experiments were performed with chromatin from samples taken before (time point 0) and every 30 min after Dex treatment for 3 h. Positions of amplicons used in the ChIP analysis are shown in Figure 5A. Data were normalized as in Figure 5B and are shown as the mean of a representative experiment.
(C) Signals for the histone mark H3K27me3 in Dex-treated *35S$_{pro}$:CO:GR* plants. Data are based on the same chromatin extract and analysis as used in **(B)**.
(D) H3K9K14ac signals along the *FT* locus before and after *FT* induction. The experiment is based on the same chromatin extract as used in **(B)**. Signals were normalized as in Figure 5D.
Data in **(B)** to **(D)** are shown as the mean of a representative experiment. Error bars show the 95% confidence interval of three technical replicates.

constructs in a *lhp1* mutant background revealed that repression of *FT* in the middle vein and the proximal half of the leaf by LHP1 is mediated through promoter sequences 1.0 to 4.0 kb upstream of *FT*. As a 4.0-kb *FT* promoter cannot be induced by high levels of CO, *FT* repression in the midvein by LHP1 seems to be needed to neutralize one or several unknown activators of *FT* in this tissue (see model in Figure 7B). The *FT* locus is widely covered by the repressive H3K27me3 mark and LHP1 (Turck et al., 2007; Zhang et al., 2007b), but the conserved *block C* that is crucial for CO responsiveness coincides with a locally H3K27me3 and LHP1 poor region that may be part of a regulatory mechanism maintaining a window of constitutively open chromatin accessible to regulatory factors (Figure 7A).

Going along with the idea that LHP1 binding and presence of the repressive H3K27me3 mark interferes with the access of transcription factors to the *FT* promoter, it is remarkable that LHP1 binding is reduced in *35S$_{pro}$:CO* plants throughout the locus (Figure 5B). The loss of LHP1, together with the increased H3K9K14ac (Figure 5D), could result in a more permissive chromatin structure that facilitates the access of other transcriptional regulators to elements that are usually repressed and contribute to high *FT* expression in the midvein in *35S$_{pro}$:CO* plants (Figure 7B). In contrast with LHP1, the H3K27me3 mark does not differ in the same conditions (Figure 5C). Several published results show that transcriptional activity does not always correlate with changes in H3K27me3. In plants carrying a *AGAMOUS$_{pro}$:GUS* transgene, GUS signal is obtained even when the transgene is enriched for H3K27me3 (Schubert et al., 2006). Two cold-responsive genes targeted by H3K27me3, *COR15A* and *ATGOLS3*, lose H3K27me3 with delayed kinetics compared with transcriptional induction in the cold. In addition, upon return to warmer ambient temperature, the expression of these genes is fully repressed before recovery of H3K27me3 (Kwon et al., 2009). The widely studied *FLC* locus represents an emblematic example of epigenetically maintained gene repression via a PcG-dependent mechanism. However, the structural *FLC* locus is always enriched in H3K27me3 (Turck et al., 2007; Zhang et al., 2007b), and only an increased spreading of the histone mark and presence of LHP1 after vernalization prevents *FLC* expression (Mylne et al., 2006; Sung et al., 2006; Finnegan and Dennis, 2007). The precise mechanism by which the spreading of H3K27me3 stabilizes the repression of FLC is not elucidated and could depend on the de novo condensation of a restricted regulatory region, in analogy to the situation observed

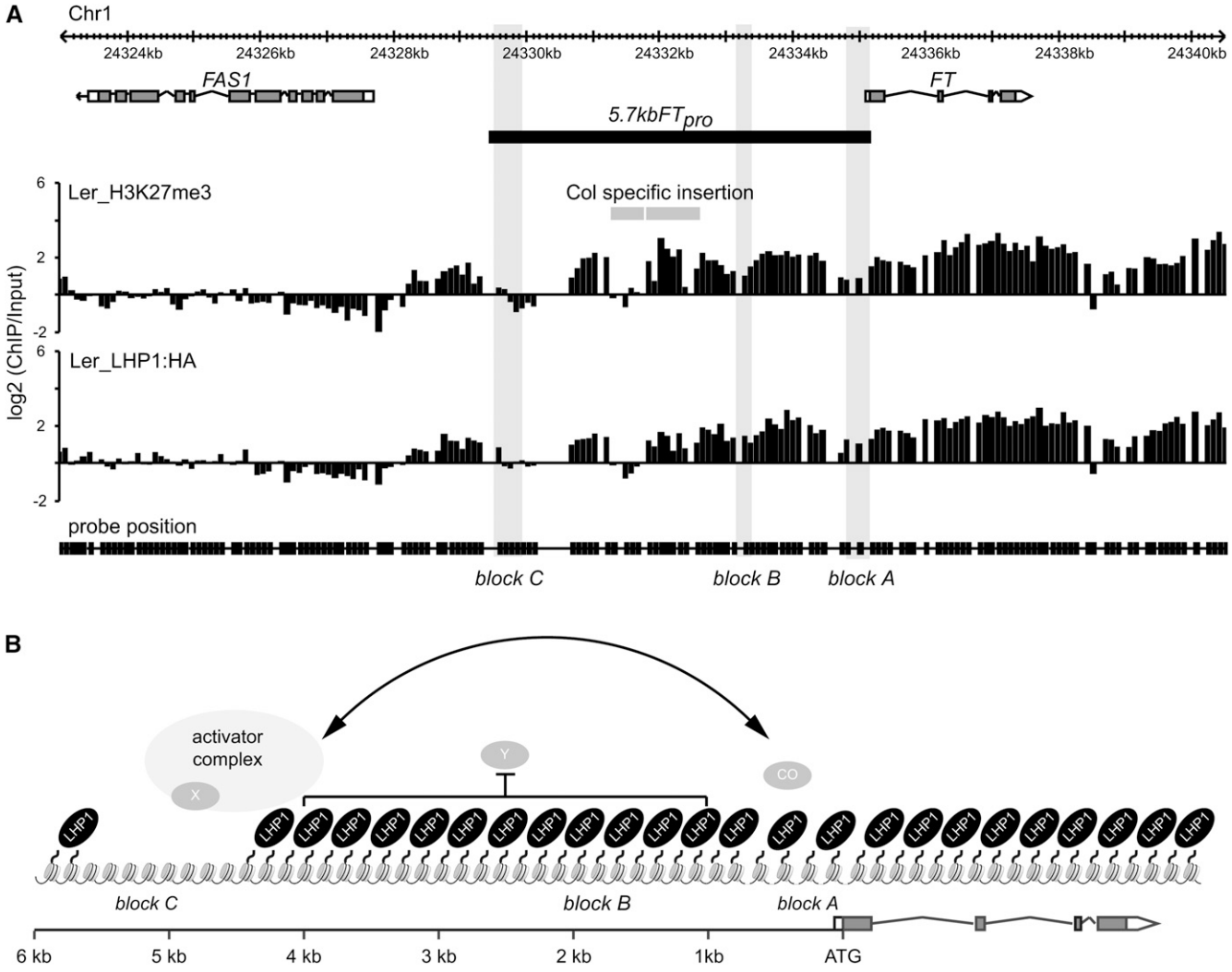

Figure 7. A Model of *FT* Transcriptional Activation Mediated through Interaction of Two Conserved and LHP1-Depleted Regions.

(A) Schematic diagram of the distribution of H3K27me3 chromatin mark and LHP1:HA protein in $35S_{pro}$*:LHP1:HA* L*er* plants. ChIP-chip material was generated from 10-d-old seedlings grown on GM medium under LD conditions. Enrichment was calculated as the log2 ratio of ChIP sample versus input sample. Two Col-specific insertions that are not present in L*er* are depicted in gray. Light-gray areas highlight the conserved blocks upstream of *FT*.
(B) The model shows a constitutively LHP1 poor region that coincides with *block C* and might enable accessibility of transcription factors required for CO-dependent activation of *FT*. This interaction of CO with a protein partner or an activator complex might enhance CO binding DNA affinity to *block A* located in the proximal promoter. The middle part of the promoter contains response elements for one or several unknown activating factors "Y," which are specifically expressed in the midvein. The middle part of the promoter is accessible after a prolonged high expression of *FT* or when LHP1 is genetically deleted.

for the regulatory regions in the 4.0-kb promoter of *FT* (Figure 4). Clearly, transcription can take place in the presence of repressive marks, as has been previously proposed in plants and animals (Schubert et al., 2006; Schwartz and Pirrotta, 2007).

Histone acetylation has been involved with transcription initiation and elongation (Loidl, 2004; Chen and Tian, 2007; Choi and Howe, 2009) and is mostly found at promoters and the 5′-ends of transcribed units, peaking around the core promoter (Choi and Howe, 2009). In *A. thaliana*, *TOC1* and *FLC* are examples of transcriptional regulation mediated by the acetylation status (Perales and Mas, 2007; Farrona et al., 2008), and the *PetE* gene from pea (*Pisum sativum*) is hyperacetylated at *cis*-regulatory regions upstream of the transcriptional start site when highly expressed (Chua et al., 2003). We found two hyperacetylated regions at the *FT* distal and proximal *FT* promoter when this gene is constitutively highly expressed (Figure 5D), indicating that those regions might have a similar chromatin structure that facilitates *FT* expression.

Nonetheless, chromatin changes in response to *FT* induction seem to be a delayed response and not a prerequisite for *FT*

transcription because no changes were observed preceding *FT* expression in an inducible experimental setup (Figure 6). In *A. thaliana*, there are only a few reports on short-term chromatin modifications upon transcriptional activation. Using an estrogen receptor-based inducible system, Ng et al. (2006) showed that acetylation of H3K9 coincides with activation of the *phas* promoter. However, again, the results indicate that epigenetic changes are more the consequence of gene expression rather than the cause. Similar data were obtained in the analysis of the chromatin changes induced by the circadian clock in *TOC1* expression (Perales and Mas, 2007).

In conclusion, the role of chromatin-mediated repression at *FT* is more one of expression tuning than a means to switch from a transcriptional off to an on state and vice versa. Induction of *FT* depends on an interplay between the proximal promoter and a conserved distal regulatory region that has a more accessible chromatin environment. Strong and persistent activation of *FT* results in a loss of repressive chromatin from the entire *FT* promoter. As a result, new access to chromatin-repressed *cis*-elements results in an extended expression domain for *FT* within the phloem and ultimately to an accelerated flowering response.

METHODS

Plant Material and Plant Growth Conditions

Arabidopsis thaliana plants of the accessions Col and L*er* were used as genetic background. Plants were grown at 20°C under LDs (16 h light/8 h dark), ESDs (8 h light/8 h incandescent light/8 h dark), or SDs (8 h light/16 h dark) conditions after stratification at 4°C for 2 to 4 d. Light was provided by fluorescent tubes complemented by incandescent bulbs to increase the proportion of far red light. Since high-intensity light is required for photosynthesis, plants grown in ESDs were not developmentally advanced when compared with SD-grown seedlings. Nonetheless, reduced light quantity in ESD conditions compared with LD conditions did not affect floral transition. Plants on plates were grown on GM medium supplemented with 1% (w/v) sucrose under LDs.

Flowering Time Measurement

Seeds were stratified for 3 d at 4°C on wet filter paper and then sown on soil in ESD or SDs. Flowering time was measured by scoring the number of rosette and cauline leaves on the main stem of at least 12 individuals. Data are expressed as mean ± SE. For statistical analysis, two-way analyses of variance were calculated using a general linear model with the SAS software package version 9.1.

Plasmid Constructions

FT promoter sequences were amplified from Col DNA with oligonucleotides indicated in Supplemental Table 1 online. PCR products were introduced into the GATEWAY *pDONR207* vector (Invitrogen), and absence of PCR induced mutations in the constructs was confirmed by DNA sequencing. Overlapping primer pairs were designed to introduce point mutations into the proximal *FT* promoter sequence (see Supplemental Table 1 online, mutations depicted in bold). A *Bam*HI and *Pst*I fragment from *8.1kbFT$_{pro}$-pDONR207* was replaced with the corresponding fragment containing the mutations.

To generate the binary destination vectors *GW:GUS*, *GW:LUC*, and *GW:GreenLUC*, *GUS* coding sequences from pBT10-GUS (Sprenger-Haussels and Weisshaar, 2000) and *LUC* coding sequences from *pGEM-luc*$^+$ and *pCBG68luc* vector (both Promega) were cloned into the multiple cloning site of the *GW-MCS-NOS-pGREEN* vector (Corbesier et al., 2007). The binary destination vector *GW:FTcDNA* was described by Corbesier et al. (2007). To construct control vectors for transient bombardments, the *GreenLUC* and *RedLUC* genes were excised from the Promega *pCBG68luc* and *CBRluc* vectors and introduced into pJAN. The *35S$_{pro}$:gCO-pBluescript* construct was described by Onouchi et al. (2000).

Plant Transformation and Transgenic Lines

All plasmids based on *pGREEN0229* were introduced into *Agrobacterium tumefaciens* strain GV3101 containing the helper plasmid *pSOUP* (Koncz and Schell, 1986). Plasmids were transformed into *A. thaliana* plants by the floral dip method (Clough and Bent, 1998). For *GUS* expression analysis, constructs were introduced into wild-type Col and *35S$_{pro}$:CO* Col plants (Onouchi et al., 2000) and *lhp1-1* mutant background (Larsson et al., 1998). The T-DNA insertion line *ft-10* in the Col background (Yoo et al., 2005) was used for complementation analysis.

In the T1 generation, plants carrying a *pGREEN0229* plasmid were identified on the basis of BASTA resistance. The next generation was tested for single locus insertion of the transgene based on a 3:1 segregation on GM medium containing 12 μg/mL phosphinotricin. The selected plants were segregated to obtain T3 homozygous lines for GUS expression and flowering time experiments.

For *FT$_{pro}$:GUS 35S$_{pro}$:CO* double transgenic lines, *8.1kbFT$_{pro}$:GUS*, *4.0kbFT$_{pro}$:GUS*, and *1.0kbFT$_{pro}$:GUS* Col lines were crossed with *35S$_{pro}$:CO* Col plants. Transgenic lines carrying *5.7kbFT$_{pro}$:GUS* in Col and *35S$_{pro}$:CO* background are based on independent transformations. The *35S$_{pro}$:LHP1:HA* line was previously obtained (Turck et al., 2007). The same line was crossed with a *35S$_{pro}$:CO co-2 tt-4* and a *35S$_{pro}$:CO:GR co-2 tt-4* line (Onouchi et al., 2000).

Expression Analysis

The aerial part of soil-grown plants was collected to extract total RNA with the RNeasy mini kit (Qiagen). Five micrograms of RNA was DNase treated using the DNA-free kit (Ambion) to cDNA synthesis. Quantitative real-time RT-PCR was performed using a BioRad iQ5 apparatus and SYBR Green II detection. A dilution series of a specific plasmid was used as standard for each primer pair during quantitative PCR and allowed calculation of molar ratios. *Actin* was used as a housekeeping gene. Primer sets can be found in Supplemental Table 1 online.

For GUS staining, seedlings were incubated for 30 min in 90% (v/v) acetone on ice, rinsed with 50 mM sodium phosphate buffer, pH 7.0, and incubated for 17 h at 37°C in staining solution (0.5 mg × mL^{-1} X-Gluc [5-bromo-4-chloro-3-indolyl-β-D-glucuronide], 50 mM sodium phosphate buffer, pH 7.0, 0.5 mM potassium ferrocyanide, 0.5 mM potassium ferricyanide, and 0.1% [v/v] Triton X-100). After staining, samples were washed with 50 mM sodium phosphate buffer, pH 7.0, and cleared in 70% (v/v) ethanol. The GUS histochemical staining was visualized under a light stereomicroscope (MZ 16 FA; Leica).

Phylogenetic Analysis and Transcription Factor Binding Site Identification

FT sequences from *Arabidopsis lyrata*, *Capsella rubella*, and *Brassica oleracea* were assembled using shotgun sequences available from the National Center for Biotechnology Information (http://www.ncbi.nlm.nih.gov). A BAC clone from *Brassica rapa* containing a *FT*-like gene was obtained from the Multinational *Brassica* Genome Project (http://www.brassica.info). *Arabis alpina* sequences were obtained after sequencing of Aa *FT1*, Aa *FT2*, and Aa *FT3* containing BACs using the Sanger method

(M.C. Albani and G. Coupland, unpublished data). Short sequence stretches of the promoters of *FT*-like genes from *Sisymbrium polyceratum* and *Arabis hirsuta* were amplified using PCR primers that were based on the *A. thaliana* proximal *FT* promoter sequence 5′-GTGGCTAC-CAAGTGGGAGAT-3′ and 5′-TAACTCGGGTCGGTGAAATC-3′. mVista Shuffle-LAGAN was used to create pairwise alignments of long *FT* promoter sequences from *A. thaliana*, *A. lyrata*, *B. rapa*, and the Aa *FT1* gene (http://genome.lbl.gov/vista) (Brudno et al., 2003; Frazer et al., 2004). Sequences of conserved regions were analyzed with ClustalW2 (http://www.ebi.ac.uk/Tools/clustalw2) (Larkin et al., 2007). Plant *cis*-acting regulatory DNA elements were searched through the PLACE database with a cutoff of >4 bp (http://www.dna.affrc.go.jp/PLACE) (Higo et al., 1999). Sequences and FASTA output files of mVista and ClustalW alignments can be found in Supplemental Data Set 1 online.

Transient Assays

For transient assays, 5 μg of each *35S$_{pro}$:GFP-pBluescript* and *FT$_{pro}$:LUC-pGREEN* or *35S$_{pro}$:RedLUC-pJAN* and *indicatedFT$_{pro}$:GreenLUC-pGREEN* were mixed with 5 μg of an empty vector (*pKS*) or *35S$_{pro}$:gCO-pBluescript* according to standard procedures and bombarded 5 to 10 mm long *A. thaliana* leaves of SD-grown Col plants using the Biolistic particle delivery system (PDS-1000/HE; Bio-Rad). After incubation overnight in LDs, transformed leaves were sprayed with 1 mM luciferin, and luciferase activity was detected using a Hamamatsu photon counting system. Activity of the LUC luciferase was normalized by GFP signal obtained in five different leaves. Activities of the GreenLUC and RedLUC luciferases were measured through different optical filters (LEE Filters; filter #139 primary green and filter #126 bright red). To calculate the amount of RedLUC activity measured through the green filter and vice versa, one bombardment with *35S$_{pro}$:RedLUC-pJAN* and one bombardment with *35S$_{pro}$:GreenLUC-pJAN* were only performed. The ratios of signals were calculated by a formula provided by Promega.

ChIP

For ChIP experiments performed in the *35S$_{pro}$:CO* background, 10-d-old seedlings grown on GM media under SD conditions were harvested. For the experiments in the *35S$_{pro}$:CO:GR* background, plants were grown on soil under SD conditions until day 10 when they were sprayed with a solution of 1 mM Dex and harvested just before the treatment (time 0) or every 30 min until 3 h after the treatment. ChIP experiments were performed as previously described (Searle et al., 2006) with anti-HA antibodies (H6908; Sigma-Aldrich), anti-H3K27me3 (07-449; Millipore), and H3K9K14ac antibodies (06-599; Millipore). A very low signal was detected in mock antibody precipitations and was considered as background. A small aliquot of untreated sonicated chromatin was used as the total input DNA. Normalization of LHP1:HA binding and H3K27me3 data was performed using the signal obtained at *At4g24640*, a Polycomb and LHP1-regulated gene that is not affected by photoperiod (Turck et al., 2007). H3K9K14ac data were normalized with the signal obtained at *At1g67090*, which is highly expressed and is not influenced by photoperiod. Quantitative PCR data are shown as fold enrichment over the control genes and are means of three technical replicates. At least two independent biological replicates were performed for each experiment and a representative one is shown. Primers used for ChIP-PCR are described in Supplemental Table 1 online.

ChIP-chip

Chromatin was obtained from 35S$_{pro}$:LHP1:HA L*er* seedlings grown for 10 d on GM medium under LDs and harvested at ZT0 when *FT* is not expressed. Chromatin was precipitated using anti-H3K27me3 and anti-HA antibodies. DNA was amplified by linker-mediated PRC and hybridized to two-color microarrays from Roche; input samples were hybridized as reference. The data were normalized by LOESS and averages of two biological replicates uploaded to the TAIR genome browser for visualization (see Supplemental Data Set 6 online). For a detailed description of ChIP-chip sample generation and data analysis, see Göbel et al. (2010) and Reimer and Turck (2010).

Accession Numbers

Sequence data from this article can be found in the Arabidopsis Genome Initiative data library under the following accession numbers: *AG* (*At4g18960*), *ATGOLS3* (*At1g09350*), *CIB1* (*At4g34530*), *CO* (*At5g15840*), *COR15A* (*At2g42540*), *FAS1* (*At1g65470*), *FLC* (*At5g10140*), *FT* (*At1g65480*), *LHP1* (*At5g17690*), *NF-YB2* (*At5g47640*), *NF-YB3* (*At4g14540*), *SMZ* (*At3g54990*), *SVP* (*At2g22540*), *TEM1* (*At1g25560*), *TEM2* (*At1g68840*), *TFL1* (*At5g03840*), *TOC1* (*At5g61380*), *TSF* (*At4g20370*), *A. alpina FT1*$_{pro}$ (*FN813298*), *B. rapa FT*$_{pro}$ (FN813299), *A. lyrata FT*$_{pro}$ (FN813300), *S. polyceratium FT*$_{pro}$ block A (FN813301), *C. rubella FT*$_{pro}$ block A (FN813302), *B. oleracea FT*$_{pro}$ block A (FN813303), *A. hirsuta FT*$_{pro}$ block A (FN813304), *A. alpina FT2*$_{pro}$ block A (FN813305), *A. alpina FT3*$_{pro}$ block A (FN813306), and *C. rubella FT*$_{pro}$ block C (FN813307).

Supplemental Data

The following materials are available in the online version of this article.

Supplemental Figure 1. Response to Daylength Mediated by the 8.1-kb *FT* Promoter.

Supplemental Figure 2. Spatial *FT* Expression at Different Developmental Stages.

Supplemental Figure 3. *FAS1* Expression Does Not Change in *35S$_{pro}$:CO* Plants.

Supplemental Figure 4. Nuclear Import of CO upon Dexamethasone Treatment of *35S$_{pro}$:LHP1:HA; 35S$_{pro}$:CO:GR* L*er* Plants Triggers Flowering.

Supplemental Table 1. List of Primers Used.

Supplemental Data Set 1. mVista Alignments of Col *FT$_{pro}$* and L*er* *FT$_{pro}$* Sequences (FASTA Format).

Supplemental Data Set 2. mVista Alignments of Col *FT$_{pro}$* and *Arabidopsis lyrata FT$_{pro}$* Sequences (FASTA Format).

Supplemental Data Set 3. mVista Alignments of Col *FT$_{pro}$* and *Brassica rapa FT$_{pro}$* Sequences (FASTA Format).

Supplemental Data Set 4. mVista Alignments of Col *FT$_{pro}$* and *Arabis alpina FT1$_{pro}$* Sequences (FASTA Format).

Supplemental Data Set 5. ClustalW Alignments of *FT$_{pro}$* Block A, B, and C Sequences (FASTA Format).

Supplemental Data Set 6. ChIP-chip Data for the *FT* Locus (GFF Format).

ACKNOWLEDGMENTS

We thank Markus Berns for his assistance with phylogenetic analysis, Jarod Rollins for help with statistical analysis, Doris Wagner for critical reading of the manuscript, and Anna Zakrisson-Plogander and Valentina Strizhova for the screening of the *A. alpina* BAC library and excellent technical help, respectively. We acknowledge financial support from

European Molecular Biology Organization, the Deutsche Forschungsgemeinshaft, and the Max Planck Society.

Received February 17, 2010; revised April 16, 2010; accepted May 3, 2010; published May 14, 2010.

REFERENCES

Abe, M., Kobayashi, Y., Yamamoto, S., Daimon, Y., Yamaguchi, A., Ikeda, Y., Ichinoki, H., Notaguchi, M., Goto, K., and Araki, T. (2005). FD, a bZIP protein mediating signals from the floral pathway integrator FT at the shoot apex. Science **309:** 1052–1056.

Aukerman, M.J., and Sakai, H. (2003). Regulation of flowering time and floral organ identity by a microRNA and its APETALA2-like target genes. Plant Cell **15:** 2730–2741.

Ben-Naim, O., Parnis, R.E.A., Teper-Bamnolker, P., Shalit, A., Coupland, G., Samach, A., and Lifschitz, E. (2006). The CCAAT binding factor can mediate interactions between CONSTANS-like proteins and DNA. Plant J. **46:** 462–476.

Bradley, D., Ratcliffe, O., Vincent, C., Carpenter, R., and Coen, E. (1997). Inflorescence commitment and architecture in Arabidopsis. Science **275:** 80–83.

Brudno, M., Malde, S., Poliakov, A., Do, C.B., Couronne, O., Dubchak, I., and Batzoglou, S. (2003). Glocal alignment: Finding rearrangements during alignment. Bioinformatics **19:** i54–i62.

Cai, X., Ballif, J., Endo, S., Davis, E., Liang, M., Chen, D., DeWald, D., Kreps, J., Zhu, T., and Wu, Y. (2007). A putative CCAAT-binding transcription factor is a regulator of flowering timing in Arabidopsis. Plant Physiol. **145:** 98–105.

Castillejo, C., and Pelaz, S. (2008). The balance between CONSTANS and TEMPRANILLO activities determines FT expression to trigger flowering. Curr. Biol. **18:** 1338–1343.

Chen, N.Z., Zhang, X.Q., Wei, P.C., Chen, Q.J., Ren, F., Chen, J., and Wang, X.C. (2007). AtHAP3b plays a crucial role in the regulation of flowering time in Arabidopsis during osmotic stress. J. Biochem. Mol. Biol. **40:** 1083–1089.

Chen, Z.J., and Tian, L. (2007). Roles of dynamic and reversible histone acetylation in plant development and polyploidy. Biochim. Biophys. Acta **1769:** 295–307.

Choi, J.K., and Howe, L.J. (2009). Histone acetylation: Truth of consequences? Biochem. Cell Biol. **87:** 139–150.

Chua, Y.L., Watson, L.A., and Gray, J.C. (2003). The transcriptional enhancer of the pea plastocyanin gene associates with the nuclear matrix and regulates gene expression through histone acetylation. Plant Cell **15:** 1468–1479.

Clough, S.J., and Bent, A.F. (1998). Floral dip: A simplified method for Agrobacterium-mediated transformation of *Arabidopsis thaliana*. Plant J. **16:** 735–743.

Corbesier, L., Vincent, C., Jang, S.H., Fornara, F., Fan, Q.Z., Searle, I., Giakountis, A., Farrona, S., Gissot, L., Turnbull, C., and Coupland, G. (2007). FT protein movement contributes to long-distance signaling in floral induction of Arabidopsis. Science **316:** 1030–1033.

Degenhardt, J., and Tobin, E.M. (1996). A DNA binding activity for one of two closely defined phytochrome regulatory elements in an Lhcb promoter is more abundant in etiolated than in green plants. Plant Cell **8:** 31–41.

Del Olmo, I., Lopez-Gonzalez, L., Martin-Trillo, M.M., Martinez-Zapater, J.M., Pineiro, M., and Jarillo, J.A. (2009). EARLY IN SHORT DAYS 7 (ESD7) encodes the catalytic subunit of DNA polymerase epsilon and is required for flowering repression through a mechanism involving epigenetic gene silencing. Plant J. **61:** 623–636.

Exner, V., Aichinger, E., Shu, H., Wildhaber, T., Alfarano, P., Caflisch, A., Gruissem, W., Koehler, C., and Hennig, L. (2009). The chromodomain of LIKE HETEROCHROMATIN PROTEIN 1 is essential for H3K27me3 binding and function during Arabidopsis development. PLoS One **4:** e5335.

Farrona, S., Coupland, G., and Turck, F. (2008). The impact of chromatin regulation on the floral transition. Semin. Cell Dev. Biol. **19:** 560–573.

Finnegan, E.J., and Dennis, E.S. (2007). Vernalization-induced trimethylation of histone H3 lysine 27 at FLC is not maintained in mitotically quiescent cells. Curr. Biol. **17:** 1978–1983.

Frazer, K.A., Pachter, L., Poliakov, A., Rubin, E.M., and Dubchak, I. (2004). VISTA: Computational tools for comparative genomics. Nucleic Acids Res. **32:** W273–279.

Göbel, U., Reimer, J., and Turck, F. (2010). Genome-wide mapping of protein-DNA interaction by chromatin immunoprecipitation and DNA microarray hybridization (ChIP-chip). Part B: ChIP-chip data analysis. Methods Mol. Biol. **631:** 161–184.

Hebbar, P.B., and Archer, T.K. (2007). Chromatin-dependent cooperativity between site-specific transcription factors in vivo. J. Biol. Chem. **282:** 8284–8291.

Hedman, H., Kallman, T., and Lagercrantz, U. (2009). Early evolution of the MFT-like gene family in plants. Plant Mol. Biol. **70:** 359–369.

Higo, K., Ugawa, Y., Iwamoto, M., and Korenaga, T. (1999). Plant cis-acting regulatory DNA elements (PLACE) database: 1999. Nucleic Acids Res. **27:** 297–300.

Jaeger, K.E., and Wigge, P.A. (2007). FT protein acts as a long-range signal in Arabidopsis. Curr. Biol. **17:** 1050–1054.

Jang, S., Torti, S., and Coupland, G. (2009). Genetic and spatial interactions between FT, TSF and SVP during the early stages of floral induction in Arabidopsis. Plant J. **60:** 614–625.

Jeong, J.H., Song, H.R., Ko, J.H., Jeong, Y.M., Kwon, Y.E., Seol, J.H., Amasino, R.M., Noh, B., and Noh, Y.S. (2009). Repression of FLOWERING LOCUS T chromatin by functionally redundant histone H3 lysine 4 demethylases in Arabidopsis. PLoS One **4:** e8033.

Kardailsky, I., Shukla, V.K., Ahn, J.H., Dagenais, N., Christensen, S.K., Nguyen, J.T., Chory, J., Harrison, M.J., and Weigel, D. (1999). Activation tagging of the floral inducer FT. Science **286:** 1962–1965.

Kobayashi, Y., Kaya, H., Goto, K., Iwabuchi, M., and Araki, T. (1999). A pair of related genes with antagonistic roles in mediating flowering signals. Science **286:** 1960–1962.

Koncz, C., and Schell, J. (1986). The promoter of Tl-DNA gene 5 controls the tissue-specific expression of chimeric genes carried by a novel type of Agrobacterium binary vector. Mol. Gen. Genet. **204:** 383–396.

Koornneef, M., Hanhart, C.J., and van der Veen, J.H. (1991). A genetic and physiological analysis of late flowering mutants in *Arabidopsis thaliana*. Mol. Gen. Genet. **229:** 57–66.

Kotake, T., Takada, S., Nakahigashi, K., Ohto, M., and Goto, K. (2003). Arabidopsis TERMINAL FLOWER 2 gene encodes a heterochromatin protein 1 homolog and represses both FLOWERING LOCUS T to regulate flowering time and several floral homeotic genes. Plant Cell Physiol. **44:** 555–564.

Kumimoto, R.W., Adam, L., Hymus, G.J., Repetti, P.P., Reuber, T.L., Marion, C.M., Hempel, F.D., and Ratcliffe, O.J. (2008). The Nuclear Factor Y subunits NF-YB2 and NF-YB3 play additive roles in the promotion of flowering by inductive long-day photoperiods in Arabidopsis. Planta **228:** 709–723.

Kwon, C.S., Lee, D., Choi, G., and Chung, W.I. (2009). Histone occupancy-dependent and -independent removal of H3K27 trimethylation at cold-responsive genes in Arabidopsis. Plant J. **60:** 112–121.

Larkin, M.A., et al. (2007). Clustal W and Clustal X version 2.0. Bioinformatics **23:** 2947–2948.

Larsson, A.S., Landberg, K., and Meeks-Wagner, D.R. (1998). The TERMINAL FLOWER2 (TFL2) gene controls the reproductive transition and meristem identity in *Arabidopsis thaliana*. Genetics **149:** 597–605.

Laubinger, S., Marchal, V., Gentilhomme, J., Wenkel, S., Adrian, J., Jang, S., Kulajta, C., Braun, H., Coupland, G., and Hoecker, U. (2006). Arabidopsis SPA proteins regulate photoperiodic flowering and interact with the floral inducer CONSTANS to regulate its stability. Development **133:** 3213–3222.

Li, D., Liu, C., Shen, L., Wu, Y., Chen, H., Robertson, M., Helliwell, C.A., Ito, T., Meyerowitz, E., and Yu, H. (2008). A repressor complex governs the integration of flowering signals in Arabidopsis. Dev. Cell **15:** 110–120.

Liu, H., Yu, X., Li, K., Klejnot, J., Yang, H., Lisiero, D., and Lin, C. (2008). Photoexcited CRY2 interacts with CIB1 to regulate transcription and floral initiation in Arabidopsis. Science **322:** 1535–1539.

Loidl, P. (2004). A plant dialect of the histone language. Trends Plant Sci. **9:** 84–90.

Luo, M., Platten, D., Chaudhury, A., Peacock, W.J., and Dennis, E.S. (2009). Expression, imprinting, and evolution of rice homologs of the polycomb group genes. Mol. Plant **2:** 711–723.

Mantovani, R. (1999). The molecular biology of the CCAAT-binding factor NF-Y. Gene **239:** 15–27.

Mathieu, J., Warthmann, N., Kuttner, F., and Schmid, M. (2007). Export of FT protein from phloem companion cells is sufficient for floral induction in Arabidopsis. Curr. Biol. **17:** 1055–1060.

Mathieu, J., Yant, L.J., Murdter, F., Kuttner, F., and Schmid, M. (2009). Repression of flowering by the miR172 target SMZ. PLoS Biol. **7:** e1000148.

McNabb, D.S., and Pinto, I. (2005). Assembly of the Hap2p/Hap3p/Hap4p/Hap5p-DNA complex in *Saccharomyces cerevisiae*. Eukaryot. Cell **4:** 1829–1839.

Michaels, S.D., Himelblau, E., Kim, S.Y., Schomburg, F.M., and Amasino, R.M. (2005). Integration of flowering signals in winter-annual Arabidopsis. Plant Physiol. **137:** 149–156.

Mylne, J.S., Barrett, L., Tessadori, F., Mesnage, S., Johnson, L., Bernatavichute, Y.V., Jacobsen, S.E., Fransz, P., and Dean, C. (2006). LHP1, the Arabidopsis homologue of HETEROCHROMATIN PROTEIN1, is required for epigenetic silencing of FLC. Proc. Natl. Acad. Sci. USA **103:** 5012–5017.

Nakahigashi, K., Jasencakova, Z., Schubert, I., and Goto, K. (2005). The Arabidopsis HETEROCHROMATIN PROTEIN1 homolog (TERMINAL FLOWER2) silences genes within the euchromatic region but not genes positioned in heterochromatin. Plant Cell Physiol. **46:** 1747–1756.

Ng, D.W.K., Chandrasekharan, M.B., and Hall, T.C. (2006). Ordered histone modifications are associated with transcriptional poising and activation of the phaseolin promoter. Plant Cell **18:** 119–132.

Notaguchi, M., Abe, M., Kimura, T., Daimon, Y., Kobayashi, T., Yamaguchi, A., Tomita, Y., Dohi, K., Mori, M., and Araki, T. (2008). Long-distance, graft-transmissible action of Arabidopsis FLOWERING LOCUS T protein to promote flowering. Plant Cell Physiol. **49:** 1645–1658.

Onouchi, H., Igeno, M.I., Perilleux, C., Graves, K., and Coupland, G. (2000). Mutagenesis of plants overexpressing CONSTANS demonstrates novel interactions among *Arabidopsis* flowering-time genes. Plant Cell **12:** 885–900.

Perales, M., and Mas, P. (2007). A functional link between rhythmic changes in chromatin structure and the *Arabidopsis* biological clock. Plant Cell **19:** 2111–2123.

Putterill, J., Robson, F., Lee, K., Simon, R., and Coupland, G. (1995). The constans gene of Arabidopsis promotes flowering and encodes a protein showing similarities to zinc-finger transcription factors. Cell **80:** 847–857.

Reimer, J.J., and Turck, F. (2010). Genome-wide mapping of protein-DNA interaction by chromatin immunoprecipitation and DNA microarray hybridization (ChIP-chip). Part A: ChIP-chip molecular methods. Methods Mol. Biol. **631:** 139–160.

Robson, F., Costa, M.M.R., Hepworth, S.R., Vizir, I., Pineiro, M., Putterill, J., and Coupland, G. (2001). Functional importance of conserved domains in the flowering-time gene CONSTANS demonstrated by analysis of mutant alleles and transgenic plants. Plant J. **28:** 619–631.

Samach, A., Onouchi, H., Gold, S.E., Ditta, G.S., Schwarz-Sommer, Z., Yanofsky, M.F., and Coupland, G. (2000). Distinct roles of CONSTANS target genes in reproductive development of Arabidopsis. Science **288:** 1613–1616.

Schatlowski, N., Creasey, K., Goodrich, J., and Schubert, D. (2008). Keeping plants in shape: Polycomb-group genes and histone methylation. Semin. Cell Dev. Biol. **19:** 547–553.

Schubert, D., Primavesi, L., Bishopp, A., Roberts, G., Doonan, J., Jenuwein, T., and Goodrich, J. (2006). Silencing by plant Polycomb-group genes requires dispersed trimethylation of histone H3 at lysine 27. EMBO J. **25:** 4638–4649.

Schuettengruber, B., Chourrout, D., Vervoort, M., Leblanc, B., and Cavalli, G. (2007). Genome regulation by polycomb and trithorax proteins. Cell **128:** 735–745.

Schwartz, Y.B., and Pirrotta, V. (2007). Polycomb silencing mechanisms and the management of genomic programmes. Nat. Rev. Genet. **8:** 9–22.

Searle, I., He, Y.H., Turck, F., Vincent, C., Fornara, F., Krober, S., Amasino, R.A., and Coupland, G. (2006). The transcription factor FLC confers a flowering response to vernalization by repressing meristem competence and systemic signaling in Arabidopsis. Genes Dev. **20:** 898–912.

Shannon, S., and Meekswagner, D.R. (1991). A mutation in the Arabidopsis TFL1 gene affects inflorescence meristem development. Plant Cell **3:** 877–892.

Song, Y., Song, N., Shin, S., Kim, H., Yun, D., Lim, C., Lee, S., Kang, K., and Hong, J. (2008). Isolation of CONSTANS as a TGA4/OBF4 interacting protein. Mol. Cells **25:** 559–565.

Sprenger-Haussels, M., and Weisshaar, B. (2000). Transactivation properties of parsley proline-rich bZIP transcription factors. Plant J. **22:** 1–8.

Suarez-Lopez, P., Wheatley, K., Robson, F., Onouchi, H., Valverde, F., and Coupland, G. (2001). CONSTANS mediates between the circadian clock and the control of flowering in Arabidopsis. Nature **410:** 1116–1120.

Sung, S.B., He, Y.H., Eshoo, T.W., Tamada, Y., Johnson, L., Nakahigashi, K., Goto, K., Jacobsen, S.E., and Amasino, R.M. (2006). Epigenetic maintenance of the vernalized state in *Arabidopsis thaliana* requires LIKE HETEROCHROMATIN PROTEIN 1. Nat. Genet. **38:** 706–710.

Takada, S., and Goto, K. (2003). TERMINAL FLOWER2, an *Arabidopsis* homolog of HETEROCHROMATIN PROTEIN1, counteracts the activation of FLOWERING LOCUS T by CONSTANS in the vascular tissues of leaves to regulate flowering time. Plant Cell **15:** 2856–2865.

Terzaghi, W.B., and Cashmore, A.R. (1995). Light-regulated transcription. Annu. Rev. Plant Physiol. Plant Mol. Biol. **46:** 445–474.

Turck, F., Fornara, F., and Coupland, G. (2008). Regulation and identity of florigen: FLOWERING LOCUS T moves center stage. Annu. Rev. Plant Biol. **59:** 573–594.

Turck, F., Roudier, F., Farrona, S., Martin-Magniette, M.L., Guillaume, E., Buisine, N., Gagnot, S., Martienssen, R.A., Coupland, G., and Colot, V. (2007). Arabidopsis TFL2/LHP1 specifically associates with genes marked by trimethylation of histone H3 lysine 27. PLoS Genet. **3:** 855–866.

Valverde, F., Mouradov, A., Soppe, W., Ravenscroft, D., Samach, A., and Coupland, G. (2004). Photoreceptor regulation of CONSTANS protein in photoperiodic flowering. Science **303:** 1003–1006.

Vavouri, T., and Elgar, G. (2005). Prediction of cis-regulatory elements using binding site matrices - The successes, the failures and the reasons for both. Curr. Opin. Genet. Dev. **15:** 395–402.

Wenkel, S., Turck, F., Singer, K., Gissot, L., Le Gourrierec, J., Samach, A., and Coupland, G. (2006). CONSTANS and the CCAAT box binding complex share a functionally important domain and interact to regulate flowering of *Arabidopsis*. Plant Cell **18:** 2971–2984.

Wigge, P.A., Kim, M.C., Jaeger, K.E., Busch, W., Schmid, M., Lohmann, J.U., and Weigel, D. (2005). Integration of spatial and temporal information during floral induction in Arabidopsis. Science **309:** 1056–1059.

Xu, L., and Shen, W.-H. (2008). Polycomb silencing of KNOX genes confines shoot stem cell niches in Arabidopsis. Curr. Biol. **18:** 1966–1971.

Yamaguchi, A., Kobayashi, Y., Goto, K., Abe, M., and Araki, T. (2005). TWIN SISTER OF FT (TSF) acts as a floral pathway integrator redundantly with FT. Plant Cell Physiol. **46:** 1175–1189.

Yoo, S.K., Chung, K.S., Kim, J., Lee, J.H., Hong, S.M., Yoo, S.J., Yoo, S.Y., Lee, J.S., and Ahn, J.H. (2005). CONSTANS activates SUPPRESSOR OF OVEREXPRESSION OF CONSTANS 1 through FLOWERING LOCUS T to promote flowering in Arabidopsis. Plant Physiol. **139:** 770–778.

Zhang, X., Clarenz, O., Cokus, S., Bernatavichute, Y.V., Pellegrini, M., Goodrich, J., and Jacobsen, S.E. (2007b). Whole-genome analysis of histone H3 lysine 27 trimethylation in Arabidopsis. PLoS Biol. **5:** e129.

Zhang, X., Germann, S., Blus, B.J., Khorasanizadeh, S., Gaudin, V., and Jacobsen, S.E. (2007a). The Arabidopsis LHP1 protein colocalizes with histone H3 Lys27 trimethylation. Nat. Struct. Mol. Biol. **14:** 869–871.